इंटरनेट मानक

Disclosure to Promote the Right To Information

Whereas the Parliament of India has set out to provide a practical regime of right to information for citizens to secure access to information under the control of public authorities, in order to promote transparency and accountability in the working of every public authority, and whereas the attached publication of the Bureau of Indian Standards is of particular interest to the public, particularly disadvantaged communities and those engaged in the pursuit of education and knowledge, the attached public safety standard is made available to promote the timely dissemination of this information in an accurate manner to the public.

"जानने का अधिकार, जीने का अधिकार"
Mazdoor Kisan Shakti Sangathan
"The Right to Information, The Right to Live"

"पुराने को छोड नये के तरफ"
Jawaharlal Nehru
"Step Out From the Old to the New"

IS 12233-1-2 (1987): Electromagnetic interference characteristics of overhead power lines and high-voltage equipment, Part 1: Description of phenomena, Section 2: Effects of corona from conductors [LITD 9: Electromagnetic Compatibility]

"ज्ञान से एक नये भारत का निर्माण"
Satyanarayan Gangaram Pitroda
"Invent a New India Using Knowledge"

Act Number 22 of 2005
The Indian Parliament
RIGHT TO INFORMATION

Made Available By
Public.Resource.Org

"ज्ञान एक ऐसा खजाना है जो कभी चुराया नहीं जा सकता है"
Bhartṛhari—Nītiśatakam
"Knowledge is such a treasure which cannot be stolen"

BLANK PAGE

BRUTUM FULMEN

IGNORANTIA JURIS NON EXCUSAT

PROTECTED BY COPYRIGHT

(Reaffirmed 2003)

Indian Standard

ELECTROMAGNETIC INTERFERENCE CHARACTERISTICS OF OVERHEAD POWER LINES AND HIGH VOLTAGE EQUIPMENT

PART 1 DESCRIPTION OF PHENOMENA

Section 2 Effects of Corona from Conductors

UDC 621·391·823 [621·396] : 621·315·1

© *Copyright* 1988

BUREAU OF INDIAN STANDARDS
MANAK BHAVAN, 9 BAHADUR SHAH ZAFAR MARG
NEW DELHI 110002

Gr 7 *June* 1988

Indian Standard

ELECTROMAGNETIC INTERFERENCE CHARACTERISTICS OF OVERHEAD POWER LINES AND HIGH VOLTAGE EQUIPMENT

PART 1 DESCRIPTION OF PHENOMENA

Section 2 Effects of Corona from Conductors

Electromagnetic Compatibility Sectional Committee, LTDC 22

Chairman	*Representing*
DR M. K. RAO	Wireless Planning and Co-ordination Wing (Ministry of Communication), New Delhi
Members	
SHRI VENKAT SUBRAMANIAN (*Alternate* to Dr M. K. Rao)	
DR V. K. AGARWAL	National Physical Laboratory (CSIR), New Delhi
SHRI V. K. RUSTOGI (*Alternate*)	
SHRI M. A. BAQUI	Electronics Corporation of India Ltd, Hyderabad
SHRI V. V. SURYANARAYANA (*Alternate*)	
DR T. A. R. BHAT	Indian Institute of Technology, Madras
SHRI DALJIT SINGH	Overseas Communications Services, Bombay
SHRI J. B. DANWAR	National Airport Authority, New Delhi
SHRI K. C. GOSWAMY (*Alternate*)	
LT-COL (DR) G. K. DEB	Ministry of Defence (R & D) (LRDE) Bangalore
SHRI K. M. SAHEBU (*Alternate*)	
SHRI U. C. DIMRI	Indian Radiological Association, New Delhi
DIRECTOR (PROTECTION & INSTRUMENTATION)	Central Electricity Authority, New Delhi
DIRECTOR (SUB-STATION) (*Alternate*)	
SHRI A. K. DUBEY	Electrical Appliances Manufacturers' Association, Delhi
SHRI Y. P. SURI (*Alternate*)	
SHRI K. L. GARG	Directorate General of Supplies and Disposals, New Delhi
SHRI R. V. NARAYANAN (*Alternate*)	
SHRI J. GUPTA	Pieco Electronics and Electricals Ltd, Pune
SHRI K. RAJENDRAN (*Alternate*)	

(*Continued on page* 2)

© *Copyright* 1988
BUREAU OF INDIAN STANDARDS
This publication is protected under the *Indian Copyright Act* (XIV of 1957) and reproduction in whole or in part by any means except with written permission of the publisher shall be deemed to be an infringement of copyright under the said Act.

(*Continued from page* 1)

Members	*Representing*
JOINT DIRECTOR	Research, Design & Standards Organization, Lucknow
JOINT DIRECTOR STANDARDS (S & T)/ TE (INV) (*Alternate*)	
COL KRISHAN LAL	Ministry of Defence (DGI)
SHRI N. CHANDERPAL (*Alternate*)	
SHRI PRATAP KUMAR	Directorate of Technical Development and Production (Air), New Delhi
SHRI C. M. KRISHNAMURTHY (*Alternate*)	
PROF S. N. MITRA	Institution of Electronics and Telecommunication Engineers (IETE), New Delhi
COL J. C. ANAND (RETED) (*Alternate*)	
SHRI S. MUTHUSWAMY	Department of Telecommunication, New Delhi
SHRI ASHOK GOLAS (*Alternate*)	
SHRI W. V. B. RAMALINGAM	Directorate General of All India Radio, New Delhi
SHRI T. C. RAMDORAI (*Alternate*)	
DR N. RAMESH	NGEF Ltd, Bangalore
SHRI ROY ABRAHAM (*Alternate*)	
SHRI K. J. MOHAN RAO	Directorate of Co-ordination (Police Wireless), New Delhi
SHRI R. P. MATHUR (*Alternate*)	
SHRI M. L. SHARMA	Indian Telephone Industries Ltd, Bangalore
SHRI N. KRISHNAKUTTY (*Alternate*)	
DR B. K. SINHA	Department of Electronics, New Delhi
SHRI R. K. ARORA (*Alternate*)	
SHRI T. N. SRIVASTAVA	Automotive Research Association of India, Pune
SHRI A. B. KOMAWAR (*Alternate*)	
SHRI K. R. SURESH	Bharat Electronics Ltd, Jalahalli, Bangalore
SHRI VIRENDRA VIJAY	Directorate General of Doordarshan, New Delhi
SHRI C. D. BANERJI (*Alternate*)	
DIRECTOR (ELECTRONICS)	Director General, BIS (*Ex-officio Member*)

Secretary

SHRI D. K. NAYYAR
Deputy Director (Electronics), BIS

Indian Standard

ELECTROMAGNETIC INTERFERENCE CHARACTERISTICS OF OVERHEAD POWER LINES AND HIGH VOLTAGE EQUIPMENT

PART 1 DESCRIPTION OF PHENOMENA

Section 2 Effects of Corona from Conductors

0. FOREWORD

0.1 This Indian Standard (Part 1/Sec 2) was adopted by the Bureau of Indian Standards on 31 July 1987, after the draft finalized by the Electromagnetic Compatibility Sectional Committee had been approved by the Electronics and Telecommunication Division Council.

0.2 The purpose of the series of Part 1 of this standard is to discuss the physical phenomena involved in the generation of electromagnetic noise fields. This also includes the main properties of such fields and their numerical values.

0.3 The technical data given in these standards will be useful aid to overhead line designers and also to any one concerned with checking of electromagnetic noise performance of a line to ensure satisfactory protection of wanted electromagnetic signals.

0.3.1 The technical data should facilitate the use of the recommendations which will be given in Parts 2 and 3. These parts comprising different sections are proposed to be issued as given below:

Part 1 Description of phenomena

Part 2 Methods of measurement and procedure of determining limits

Part 3 Code of practice for minimizing the generation of radio noise

0.4 This standard is proposed to be issued in the following sections which would clarify only one aspect over the electromagnetic interference due to overhead power lines and high voltage equipment:

Section 1 Radio noise from power lines

Section 2 Effects of corona from conductors

Section 3 Radio noise levels due to insulators, fittings and sub-station equipment (excluding bad contacts)

Section 4 Sparking due to bad contacts

Section 5 Special DC effects

0.5 This standard has been largely based on CISPR Publication 18 - 1 (First Edition - 1982) 'Radio interference characteristics of overhead power lines and high voltage equipment, Part 1 Description of phenomena', issued by the International Special Committee on Radio Interference of the International Electrotechnical Commission (IEC).

0.6 For the purpose of deciding whether a particular requirement of this standard is complied with, the final value, observed or calculated, expressing the result of a test, shall be rounded off in accordance with IS : 2 - 1960*. The number of significant places retained in the rounded off value should be the same as that of the specified value in this standard.

---

1. SCOPE

1.1 This standard (Part 1/Sec 2) deals with radio noise generated by conductor corona which may cause interference to radio/TV reception.

1.2 The frequency range covered is 0·15 to 300 MHz.

2. TERMINOLOGY

2.0 For the purpose of this standard, the definition given in IS : 1885 (Part 36) - 1972† shall apply.

3. PHYSICAL ASPECTS OF CORONA FROM CONDUCTORS

3.1 General — The generation of radio noise by conductor corona is by means of the electrical discharge, usually called corona, and it occurs at or near the conductor surface. Corona is defined as 'a discharge with slight luminosity produced in the neighbourhood of a conductor and limited to the region surrounding the conductor in which the electric field exceeds a certain value'. Many aspects of corona discharge on lines are unknown and undefined; however, the basic physical process is that of electron multiplication or avalanche formation. The electric gradient in the vicinity of the line conductor is the highest and, if this gradient or electric stress is sufficiently high, any electrons in the air around the conductor

*Rules for rounding off numerical values (*revised*).

†Electrotechnical vocabulary: Part 36 Radio interference.

will ionize the gas molecules and electrons produced by this ionization will cause an avalanche. If an additional electron is formed in this gradient by some process from the original electron avalanche, a new avalanche is formed by this secondary process and the corona discharge is developed.

In the case of transmission line conductor, it is believed that the important secondary process is the election of electrons from gas molecules by high energy ultra-violet light (photo-ionization) generated by the original avalanche. It has been found by several investigators that the radio noise level generated when the conductor is positive is significantly greater than when the conductor is negative. In the case of a positive overhead line conductor, the cathode is so far away that cathode emission is of no consequence and the secondary process existing in this case is photo-ionization of the gas.

When streamer corona forms at a point on the conductor, two pulse fields will exist. Near the streamer a localized field is formed and along the line, the direct field is developed due to the pulses travelling down the line. For design of extra high voltage lines, only the direct field is considered significant, and the most useful measurements are made at some distance from the streamer locations on the line conductor.

3.2 Factors in Corona Generation — The possibility of a corona discharge taking place at the surface of a conductor is dependent upon several factors. These include:

a) Theoretical conductor surface voltage gradient which depends on:

   1) System voltage,

   2) Conductor diameter,

   3) Spacing of the conductor from earth and other phase conductor, and

   4) Number of conductors per phase or in the bundle.

b) Conductor diameter,

c) Conductor surface conditions, and

d) Atmospheric and weather conditions.

Each of these factors will be considered separately.

3.2.1 *Conductor Surface Voltage Gradient* — One of the most important quantities in determining the radio noise level of a line, especially when conductor corona is dominant, is the strength of electrical field in air at the surface of the conductor or surface voltage gradient.

Because of the close dependence of conductor corona on the value of this voltage gradient, it is necessary to use a method of calculation which gives the gradient with a precision of about 1 percent.

Since conductors are usually stranded, the surface voltage gradient varies about a mean value around the circumference of the conductor. However, it is customary to calculate the surface gradient for a smooth conductor, with the same overall diameter, even if an experimental stranding factor has to be introduced.

Formulae for the calculation of voltage gradient at the surface of a conductor are given in Appendix A for the simple case of a single-phase line with earth return or a monopolar dc line to the more complex three-phase multicircuit and bipolar dc lines. Usually the calculations need a matrix equation and computer programs are used for both single and multicircuit three-phase lines and the more complex high-voltage dc lines.

3.2.2 *Conductor Diameter* — The radio noise level increases with increasing conductor diameter even if the conductor surface gradient remains the same. This phenomenon is due to the fact that the decay of the electric field from the surface of a conductor decreases with increasing conductor diameter. Therefore, the electric field surrounding a large conductor can support longer corona streamers than the electric field around small conductors.

3.2.3 *Conductor Surface Conditions* — The type of a conductor, for example, circular or segmental stranding, and the condition of its surface, that is to say, the degree of smoothness or roughness, the presence or absence of pollution, water droplets, snow flakes, etc, have a strong influence on the generation of corona. A transmission line conductor when first strung will usually have higher corona activity due to surface irregularities such as aluminium burrs, bird droppings, dust, soil, mud or any other deposits causing corona even in fair weather. However, after a line is energized, the corona losses and radio noise will decrease with time. There are usually two time periods involved; the first period is the first few minutes after the conductor is energized and the corona activity is burning off the dust and other particles that have collected on the conductor before it was energized. The longer time period is needed to blacken completely a conductor which makes it look weathered and also destroys the surface grease on new conductors.

There is also evidence that as the conductor ages, the radio noise level, even during rain, will decrease. The surface of a new conductor is hydrophobic, due to the oil that is present on the surface from the manufacturing processes, and water beads form on this oily surface. As the conductor ages, its surface becomes hydrophilic whereby the surface of the conductor draws up the water drops into the strands.

3.2.4 *Atmospheric and Weather Conditions* — A reduction in the barometric pressure or an increase in the ambient temperature, or both, can reduce the air density which reduces the breakdown strength of air and thereby increases the likelihood of a corona discharge taking place on a conductor. The barometric pressure is usually important only at altitudes

above approximately 1 000 m. In areas that have sufficient rain, fog, frost or falling temperatures which can lead to the formation of ice or water droplets on the conductor, corona discharges are more likely to take place due to these conditions. Rain and snow are the cause of the highest corona activity at the surface of a conductor and can cause the radio noise level to increase by more than 20 dB compared with the noise from the same line under dry conditions. The water droplets or snow which collect on the conductor surface during a storm modify the electric field significantly, creating a large number of corona sources. Discharges may also occur when a snowflake or raindrop passes the conductor and initiates a discharge from the conductor to the particle.

4. METHODS OF INVESTIGATION OF CORONA BY CAGES AND TEST LINES

4.1 Two basic methods have been used to investigate the corona phenomena from transmission lines. These are test cages and test lines as given in subsequent clauses.

4.1.1 *Test Cages* — Test cages have been used by many experimenters to determine rapidly the excitation function of a conductor or a bundle of conductors. The excitation function is related to the current in the bundle by the following:

$$I = \tau \frac{C}{2\pi\varepsilon_0} \qquad \ldots(1)$$

where

I is the high frequency current injected into the conductor or bundle of conductors in $A/m^{\frac{1}{2}}$ C is the capacitance in F/m, τ is the excitation function in $A/m^{\frac{1}{2}}$ and ε_0 is the absolute premitivity of the air. The main advantage of the concept of the excitation function is that it is a quantity independent of the conductor capacitance per unit length.

The radio noise current in a test cage is measured using measuring apparatus complying with IS :10052 (Part 1) - 1982*. The current at one end of the conductor or bundle is passed through a high-frequency coupling circuit similar to those described. The equivalent impedance of the resistors and of the measuring instrument used in these circuits is usually made equal to the characteristic impedance of the conductor or bundle to avoid the occurrence of successive reflections.

Test cages have been found to give reproducible radio noise data under heavy rain but, under fair weather conditions, they have proved inadequate because of the relatively small number of sources per unit length of conductor under normal stress. The length of conductor in a

*Specification for eletromagnetic interference measuring apparatus and measurement methods: Part 1 Measuring apparatus in the frequency range 10 kHz to 1 GHz.

cage is generally too short to give a representation of an actual long line. Additionally, the surface condition of the conductor and meteorological conditions surrounding a short line near to the ground are not necessarily same as the conditions on an operational line.

The application of the excitation function of multi-phase lines requires the use of equation (1) in matrix form.

$$[I] = \frac{1}{2\pi\varepsilon_0} \times [C] \times [\tau] \qquad \ldots(2)$$

4.1.2 *Test Lines* — Whilst test cages are built for reasons of economy and case of testing, full-scale test lines are still being built, primarily to study corona phenomena on future UHV lines. There is no standard length for test lines. Test lines, single and three-phase ac lines and bipolar dc lines, as long as 8 km and as short as 300 m have been built.

There have been some attempts to measure the excitation function on short test lines and with some success specially on short dc test lines.

For long transmission lines, the radio noise frequency spectrum exhibits a characteristic of a steadily decreasing level with increasing frequency. However, for short test lines, this situation does not exist. Due to reflections of the radio noise voltages and currents at the line terminations, a standing-wave pattern in the frequency spectrum is created. This spectrum is characterized by sharp peaks and broad valleys, the exact form being dependent on the length of the line, the type of terminations, and the longitudinal location of the measuring point.

The approach that has been used by most investigators to correct the short-line frequency spectrum to the long-line spectrum is the 'Geometric mean method'. This correction is made by taking the geometric mean in terms of V/m of the successive maxima and minima of the short line frequency spectrum. In terms of dB V/m, the arithmetic mean is used.

This approach, strictly speaking, is only valid for the idealized case of a perfectly horizontal single phase line with terminations that appear as pure open circuits for radio frequencies. However, experimental studies show that, for all practical purposes, this approach is valid for ac and dc lines.

5. METHODS OF PREDETERMINATION

5.1 Because of the need for higher transmission voltages, a considerable amount of research has been conducted over the past 30 years, in various parts of the world, to understand the corona process. One of the primary purposes of this research was to develop methods to predetermine radio noise.

Radio noise measurements that have been conducted on short full-scale single and three-phase ac test lines on dc test lines, on operational

lines, and in the laboratory, have resulted in several empirical and semi-empirical formulae for predicting radio noise. These formulae can be used to predict the radio noise performance of different high-voltage lines, as long as the voltage and the design parameters are known. All the methods rely on experimental data either from test line, operational lines or test cages. Two basic methods have evolved over the years, the first one being analytical or semi-empirical and the second being empirical or comparative.

5.1.1 *Analytical Methods* — No purely analytical method of predicting transmission line radio noise exists. Two semi-empirical methods have been developed by Electricite de France (EDF) and Project Ultra High Voltage (UHV) in the United States of America. Both of these analytical methods rely on radio noise data from test cages and involve no highly complex analysis, and they are adequately described in the literature.

The calculation of radio noise from transmission lines using these analytical methods is a two-stage process. The excitation function is obtained from cage tests, the system of line capacitances is established and the injected noise currents per unit conductor length are calculated using equation (2). The theory of model propagation is applied to obtain the modal currents flowing in a given cross-section of the line. The attenuations of propagation of these modal currents are calculated and these currents are recombined into real high-frequency currents taking into account, the quadratic summation over the whole line length to obtain the total noise currents.

The next step is to calculate the noise field near the line, which is based on the total noise currents through the cross-section of the line, or the noise voltages on the phases. The lateral noise profile can then be obtained.

Computer programs are usually used to perform these complex calculations and such programs have been written at EDF and Project UHV.

5.1.2 *CIGRE Method* — The comparative formulae are generally quite simple and easy to use. Some of the best known formulae for ac lines are described in a CIGRE Publication and the technical literature. There are also several comparative formulae for dc lines and these are described in Section 5 of this series.

The highest precision of predetermination, using any of these formulae, is obtained by choosing long-term data from an operational reference line which uses conductors or bundles close to those being studied.

CIGRE has a more complete analysis of different predetermination methods using the data collected by the CIGRE/IEEE survey. From this analysis, they developed a new method that can be considered optional. This method is expressed by a fairly simple formula, which is given in 'Indian Standard Radio interference characteristics of

overhead power lines and high voltage equipment : Part 3 (*under consideration*).

6. CATALOGUE OF STANDARD PROFILES

6.1 A large number of measurements on operational lines, together with calculations supported by measurements on cage and test lines, have been carried out and examples of the results for a variety of line designs are given in Appendix B. The given values are valid only for lines constructed and maintained according to normal practice and not heavily polluted, as otherwise these conditions can give rise to higher radio noise levels than those due to conductor corona.

Appendix B gives the estimated value of the radio noise field which it is possible to obtain under certain well-defined conditions. It also includes references which can be used for predetermining the field that a new line may be expected to produce. It also includes, as examples, curves giving the field as a function of the distance from the line for certain types of line (*see* Fig. 1 to 11).

The appearance of a given line in the catalogue in Appendix B does not mean that this line generates an acceptable radio noise level; it gives only an indication of the order of magnitude to be expected for the given line design.

6.1.1 *Principle of Catalogue Presentation* — Radio noise measurements taken both on operational lines and test lines have indicated that the stability and reproducibility of the field due to conductor corona is most accurate under conditions of heavy and continuous rain. It should be noted that this heavy rain value may not be maximum foul-weather value, which can be a few decibels higher.

Extensive statistical surveys have also indicated that there is reasonable correlation between the heavy rain radio noise level and the 50 percent fair-weather level, though dispersion under fair-weather conditions is larger. For practical purposes; 50 percent fair-weather level is usually of greater importance, this value being derived from the heavy continuous-rain level by a reduction of between 17 and 25 dB, depending upon conductor surface conditions.

It is therefore possible to establish a catalogue of radio noise fields for certain transmission lines. For the practical use of this catalogue, three noise levels are considered, namely, the 50 percent fair-weather level and, depending on the origin of the profiles, either the heavy-rain level (20 dB higher) or the maximum foul-weather level (24 dB higher). From these reference levels, it is possible to estimate the radio noise levels for other types of weather, if the yearly statistical distribution of levels is known for the geographical area under consideration (*see*, for example, Fig. 13).

These principles are valid only for radio noise generated by conductor corona. The radio noise currents generated by other components of the line, insulator strings, fittings and so on, are not taken into consideration. These conditions are satisfied when the conductors of the line are subjected to a relatively high surface stress, in excess of, say, 14 kV rms per centimetre, when referred to smooth conductors. However, for lines whose conductors are subjected to a surface stress less than, say, 12 kV rms per centimetre, it is the radio noise from the insulators and other fittings which may, under certain conditions, predominate. Under these conditions, it is not possible to use this catalogue to predict the noise level since a good quality of insulators and fittings has been assumed.

The radio noise profiles for 225, 380 and 750 kV lines included in this catalogue were calculated by the Analig method. The profiles for 362, 525 and 765 kV lines were determined from the results of the CIGRE-IEEE survey.

The surface gradients have been calculated using the general method of potential coefficients. This method gives, with great accuracy, the electric surface gradient of each conductor of a line.

The shape of the lateral profiles of the radio noise field is essentially dependent on the conductor configuration. The distance between phases and their height above the ground have a major influence. The type of conductor or the bundle only slightly affects the shape of the profile owing to the structure of the capacitance matrix. When changing from one type of conductor to another with the same geometry, so long as the two matrices are proportional to each other, the profile will not be significantly changed. This assumption is sufficiently true to be applied in practice.

In Appendix B, profiles have been assembled for certain types of overhead power line. The influence of the number and arrangements of conductors per phase, their diameter and their voltage gradient, were taken into account merely by applying the appropriate correction to a reference profile. Thus each figure in the catalogue gives such a reference profile and a table of values and corrections applicable to other lines using other conductors and bundles.

The profiles are given for a measurement frequency of 0·5 MHz and the radio noise levels for other frequencies, 0·15 to 4 MHz can be obtained from Fig. 12.

The variations of the radio noise level, due either to climatic conditions or surface state of the conductors, can also be taken into consideration by estimated corrections to the levels of the basic profiles (*see* Fig. 13).

Examples of measurements and calculations can be found.

The catalogue is summarized in Appendix C according to the conventions agreed internationally, that is to say, the strengths of radio noise

fields are plotted as a function of distance, measured from the centre of the aerial loop to the nearest conductor of the line, using a logarithmic scale. From Fig. 14, it is seen that substantially straight lines are obtained and the field strengths at the reference distance of 20 m are obtained by interpolation.

The main radio noise levels, given in the catalogue, are listed in the table of Appendix C; from this table, it is possible to compare the levels of the various lines given in the catalogue and to predict, with sufficient accuracy for practical purposes, the field strength to be expected from a proposed line of similar design, provided the distance between a receiving aerial and the nearest conductor of the line is greater than 20 m.

APPENDIX A

(*Clause* 3.2.1)

CALCULATION OF VOLTAGE GRADIENT AT THE SURFACE OF A CONDUCTOR OF AN OVERHEAD LINE

A-1. Various methods are available for calculation of voltage gradient at the surface of a conductor of an overhead line. All these methods give very similar results for both non-bundle conductors and symmetrical bundles consisting of a small number of subconductors; up to three or four. For bundles with a greater number of subconductors and for asymmetrical bundles, the most suitable methods are those based on the principle of successive images (**3**). With the advent of digital computer, extensive use is now made of calculation programs based on these methods. For majority of line configurations, that is where the height of the conductors above ground and the spacing between phases or poles is large compared with the subconductor diameter or bundle dimensions and the subconductor spacing is large compared with the subconductor diameter, a single-image method can be used.

A-2. A further approximation to this approach is to calculate the charge on each conductor or subconductor, adopting the Maxwell potential coefficient method, and then to compute the voltage gradient at the surface of the conductor or subconductor considering only the charge on the conductor under consideration. In case of a conductor bundle, it may be represented by an equivalent single conductor which has the same capacitance as the bundle. For single conductors and symmetrical bundles with a small number of subconductors, very simple formulae can be used for determination of voltage gradient from the charge.

A-3. The average gradient, g_{av}, is obtained by applying Gauss's theorem, from which the electric field at the surface of a conductor is

equal to the surface charge density σ divided by the permittivity ϵ_0:

$$g_{av} = \frac{\sigma}{\epsilon_0} = \frac{q}{\epsilon_0 n \pi d} \quad \ldots(3)$$

where

q = surface charge per unit length;

n = number of subconductors in the bundle;

d = diameter of subconductor in centimetres; and

$\epsilon_0 = \frac{1}{36\pi\, 10^9}$, permittivity of free space, in farads per metre.

A-4. In the case of a single phase line with earth return or a monopolar dc line, the calculation of the charge q as a function of the applied voltage U is very simple since the capacitance per unit length C is given by:

$$C = \frac{2\pi\, \epsilon_0}{ln \frac{2h}{r_{eq}}}$$

where

h = height of conductor above ground in centimetres. Usually an average height is used and it is found by taking the conductor height at the tower, or the mean of the heights at the two towers of the span if the heights differ, and subtracting 2/3 of the sag at the lowest point of the conductor.

r_{eq} = radius of conductor or radius of bundle equivalent conductor in centimetres.

$r_{eq} = \frac{d}{2}$ in the case of a single conductor, and

$r_{eq} = \frac{b}{2}\, n \sqrt{\frac{nd}{b}}$ in the case of a conductor bundle

where b is the pitch-circle diameter of the subconductor.

Then

$$g_{av} = \frac{q}{\pi \varepsilon_0\, nd} = \frac{CU}{\pi \epsilon_0\, nd} = \frac{U}{\frac{nd}{2}\, ln \frac{2h}{r_{eq}}} \quad \ldots(4)$$

To obtain g_{av} in kilovolts per centimetre, U must be expressed in kilovolts and, in the case of ac lines, rms values are usually used.

A-5. In the general case of multiphase lines or multipole dc lines, the calculation of the charges on each conductor or bundle require the solution of the following set of equations:

$$[\,p\,]\,[\,q\,] = [\,U\,] \quad \ldots(5)$$

where

[q] and [U] are the one-column matrices of charges and voltages on the conductors or bundles and [p] is the square matrix of the potential coefficient of multiconductor configuration:

$$p_{ii} = \frac{I}{2\pi\epsilon_0} \ ln \ \frac{2h_i}{r_{eqi}}$$

$$p_{ij} = \frac{I}{2\pi\varepsilon_0} \ ln \ \frac{D'_{ij}}{D_{ij}}$$

where

D_{ij} = distance between conductors or bundles i and j, and

D_{ij} = distance between conductor or bundle i and ground image of conductor or bundle j.

A-6. As regards the matrix of voltages, the following elements are to be considered for the following practical cases:

a) *Single-Circuit Three-Phase Lines*

$$[U] \begin{bmatrix} U_1 \\ U_2 \\ U_3 \end{bmatrix} = U \begin{bmatrix} 1 \\ a \\ a^2 \end{bmatrix} \text{ with } a = \frac{-1}{2} + \frac{1}{2} j \sqrt{3}$$

where

U is modulus of phase-to-earth voltage of the line.

The above matrix refers to lines without an earth wire or wires. To take into account the presence of earth wires, the voltages, which are equal to zero on these wires, have to be inserted into the voltage matrix. The order of the matrix is increased but this does not present a great problem in the solution of the equation (5). However, it is possible, by dividing the matrix of potential coefficients into submatrices relating to phase conductors and earth wires and coupling matrices, to reduce to matrix order to that for a line without earth wires. The presence of the earth wires increases the voltage gradient at the conductors but, with usual configurations, this increase is relatively small; 1 to 3 percent.

b) *Multi-Circuit Three-Phase Lines*

In this case, voltage matrix (U) includes a series of elements which take into account all the phase conductors or bundles and, when present, the earth wires of the line. As an example, the voltage matrix of a double-circuit three-phase line with two earth wires is an eighth order column matrix. The corresponding potential coefficient matrix is an eighth order square matrix, the inversion of which requires the use of a suitable computer. However, a sufficient range of computer capabilities now exists for calculation of voltage gradient of any type of multi-circuit three-phase line.

It should be noted that the relative positions of corresponding phases in different circuits affect the charges on the conductors and it is

important to take them into account when calculating the gradients of a multicircuit line. For example, the flat formations of two circuits defined by 1, a, a^2 will result in higher gradients than the configuration 1, a, a^2 and a^2, a, 1.

c) *Bipolar dc Lines*

$$[U] = \begin{bmatrix} U_1 \\ U_2 \end{bmatrix} = U \begin{bmatrix} 1 \\ -1 \end{bmatrix}$$

where

U is the value of the pole-to-earth voltage.

The presence of earth wires can be taken into account in the same way as for ac three-phase lines.

A-7. The voltage gradient derived from formula (3) is an average value g_{av} around the circumference of the conductor or subconductor, in as much as it is calculated on the basis of the average charge density on the conductor $\left(\sigma = \frac{q}{n\pi d} \right)$.

For single conductors this charge density can be considered uniform around the circumference and, therefore, the gradient is assumed to be constant. For the subconductors in a bundle, the charge density is not uniform, due to mutual shielding effect of the subconductors, and the charge density and consequently the gradient, is larger towards the exterior and smaller towards the interior of the bundle.

A-8. A simplified approach to obtain the variation of this gradient around the circumference is given by the following formula:

$$g_\theta = g_{av} \left(I + \frac{(n-1)\,d}{b} \cos\theta \right)$$

where θ is the angle between:

a) the radius from the centre of a subconductor to a chosen point on the surface of the subconductor, and

b) the line passing through the centre of the bundle and the point where the maximum gradient occurs on the same subconductor.

In particular, the maximum gradient g_{max} is given by:

$$g_{max} = g_{av} \left(1 + \frac{(n-1)\,d}{b} \right)$$

APPENDIX B

(*Clauses* 6.1 *and* 6.1.1)

CATALOGUE OF PROFILES OF RADIO NOISE FIELD DUE TO CONDUCTOR CORONA FOR CERTAIN TYPES OF POWER LINES

B-1. The appearance of a given line in the catalogue does not purport that this line generates an acceptable radio noise level.

List of profiles

(These profiles refer to the middle of the spans and the levels are related to the voltage given at the top of each figure.)

Profiles	Figure
1. 225 kV lines	
Triangular formation of conductors	1 and 2
Flat formation	3
Arched formation	4
Flat (wide) formation	5
2. 362 kV lines	
Flat formation	6
3. 380 kV lines	
Flat formation	7
Arched formation	8
4. 525 kV lines	
Flat formation	9
5. 750 kV lines	
Arched formation	10
6. 765 kV lines	
Flat formation	11
Corrections:	
1. Frequency	12
2. Weather categories	13

APPENDIX C

SUMMARY OF CATALOGUE OF RADIO NOISE PROFILES

Figure No.	Voltage (kV)	Configuration	Noise field at the reference distance: D_o = 20 m 1) Heavy rain (dB/1 μV/m)	Dry weather (dB/1 μV/m)	Exponent (n) 2)
1	225	Triangular	52-60	32-40	−1.65
2	225	Triangular	54-62	34-42	−1.65
3	225	Flat	52-59	32-39	−1.65
4	225	Arched	54-60	34-40	−1.7
5	225	Flat, wide	49-57	29-37	−1.7
6	362 3)	Flat	68-72	48-52	−1.6
7	380	Flat	59-66	39-46	−1.7
8	380	Arched	60-67	40-47	−1.75
9	525 3)	Flat	63-70	43-50	−1.55
10	750	Arched 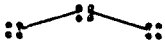	69-75	49-55	−1.65
11	765 3)	Flat	71-77	51-57	−1.55

1) Interpolated value from profiles of Fig. 1 to 11. The range (52-60 for example) takes into account the various diameters of conductors and bundle dimensions.

2) Exponent of attenuation vs distance D $\left.\begin{array}{l} \dfrac{E}{E_o}\ (\mu\ \text{V/m}) = \left(\dfrac{\ }{D_o}\right)^n \\ E\,(\text{dB}) = E_o + 20\,n \log \dfrac{D}{D_o} \end{array}\right\}$

D = direct distance in metres between the nearest conductor and the aerial of the radio noise meter.

3) The noise values are related to the maximum voltage of the line.

NOTE 1 — The average value of n is very close to −1·65. So the formula $E = E_o - 33 \log \dfrac{D}{D_o}$ can be considered as valid for all the lines.

NOTE 2 — = basic values . . . . = derived values.

As in the Original Standard, this Page is Intentionally Left Blank

Line 225 kV

Frequency 0.5 MHz	Conductors				Maximum gradients			
H min. 11 m 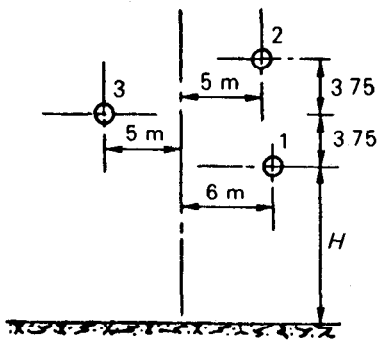	Number of conductors	Phase spacing *S* (m)	Radius of bundle *R* (mm)	Radius of conductor *r* (mm)	Phase 1 (kV eff /cm)	Phase 2 (kV eff /cm)	Phase 3 (kV eff /cm)	Level correction (dB)
	1	–	–	13.2	15.40	15.05	14.60	0
	1	–	–	15.5	13.45	13.15	12.75	–6.4
	1	–	–	16.2	12.95	12.55	12.30	–8.0

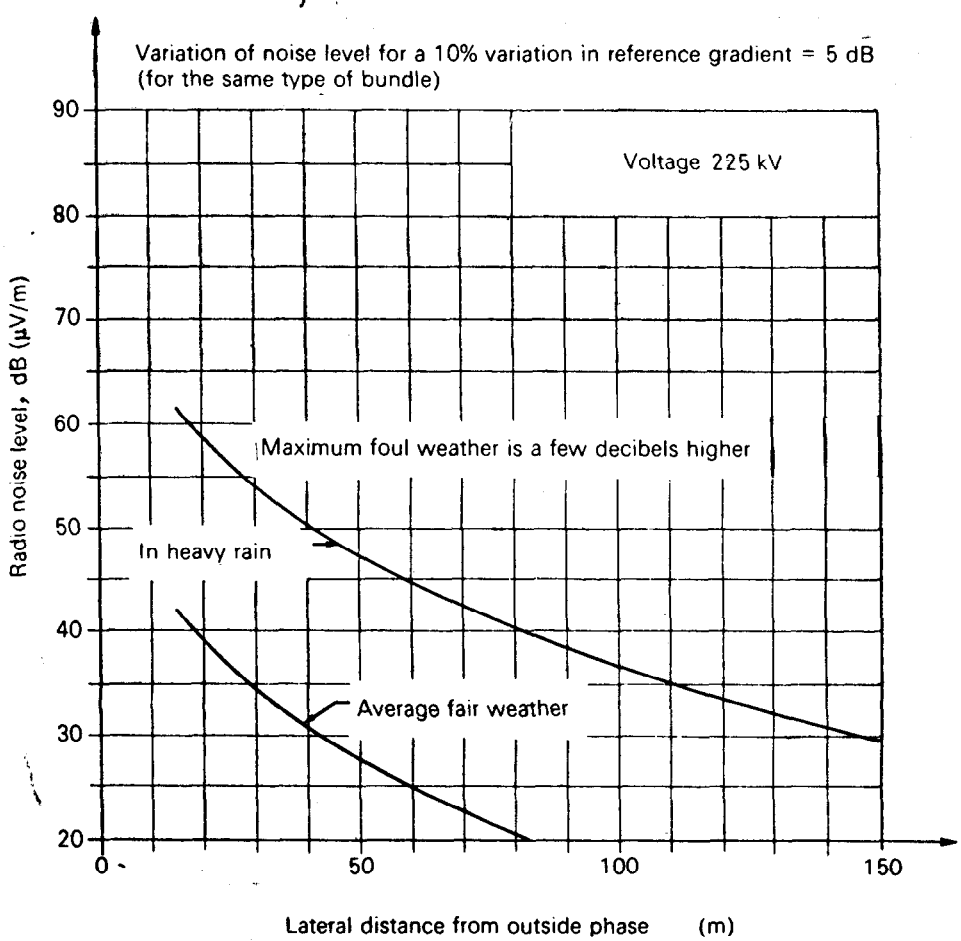

FIG. 1. — Triangular formation (1).

Line 225 kV

Frequency 0.5 MHz	Conductors				Maximum gradients			
H min. 11 m 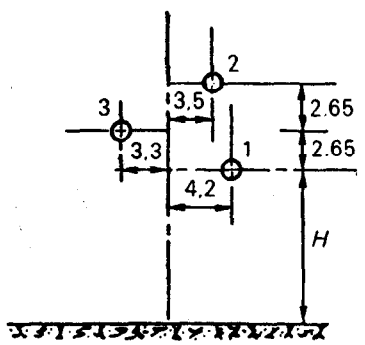	Number of conductors	Phase spacing *S* (m)	Radius of bundle *R* (mm)	Radius of conductor *r* (mm)	Phase 1 (kV eff /cm)	Phase 2 (kV eff /cm)	Phase 3 (kV eff /cm)	Level correction (dB)
	1	–	–	13.2	16.15	16.00	15.45	0
	1	–	–	15.5	14.15	14.00	13.50	−6
	1	–	–	16.2	13.65	13.50	13.00	−7.6

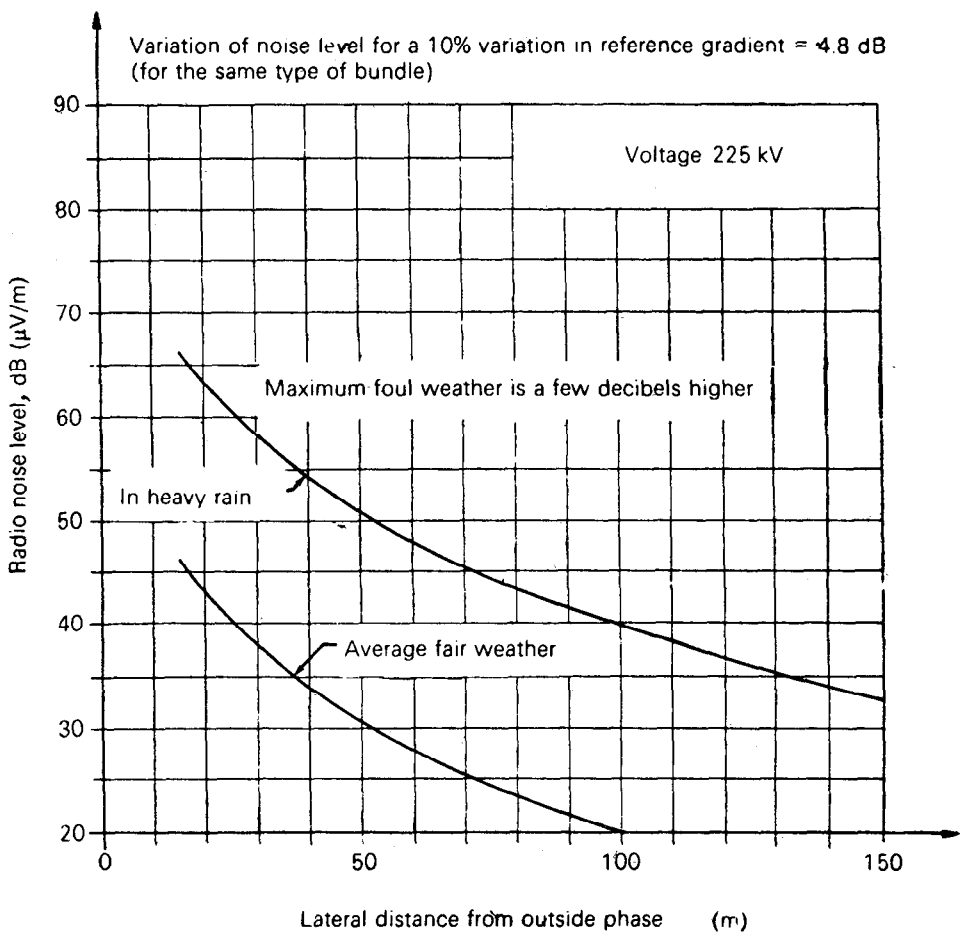

FIG. 2. — Triangular formation (2)

Line 225 kV

Frequency 0.5 MHz	Conductors				Maximum gradients			
H min. 11 m 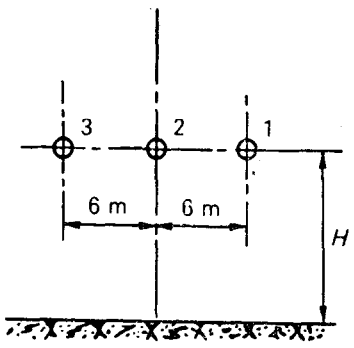	Number of conductors	Phase spacing *S* (m)	Radius of bundle *R* (mm)	Radius of conductor *r* (mm)	Phase 1 (kV eff /cm)	Phase 2 (kV eff /cm)	Phase 3 (kV eff /cm)	Level correction (dB)
	1	6	–	13.2	15.35	16.40	15.35	0
	1	6	–	15.5	13.40	14.35	13.40	−6
	1	6	–	16.2	12.90	13.85	12.90	−7.5

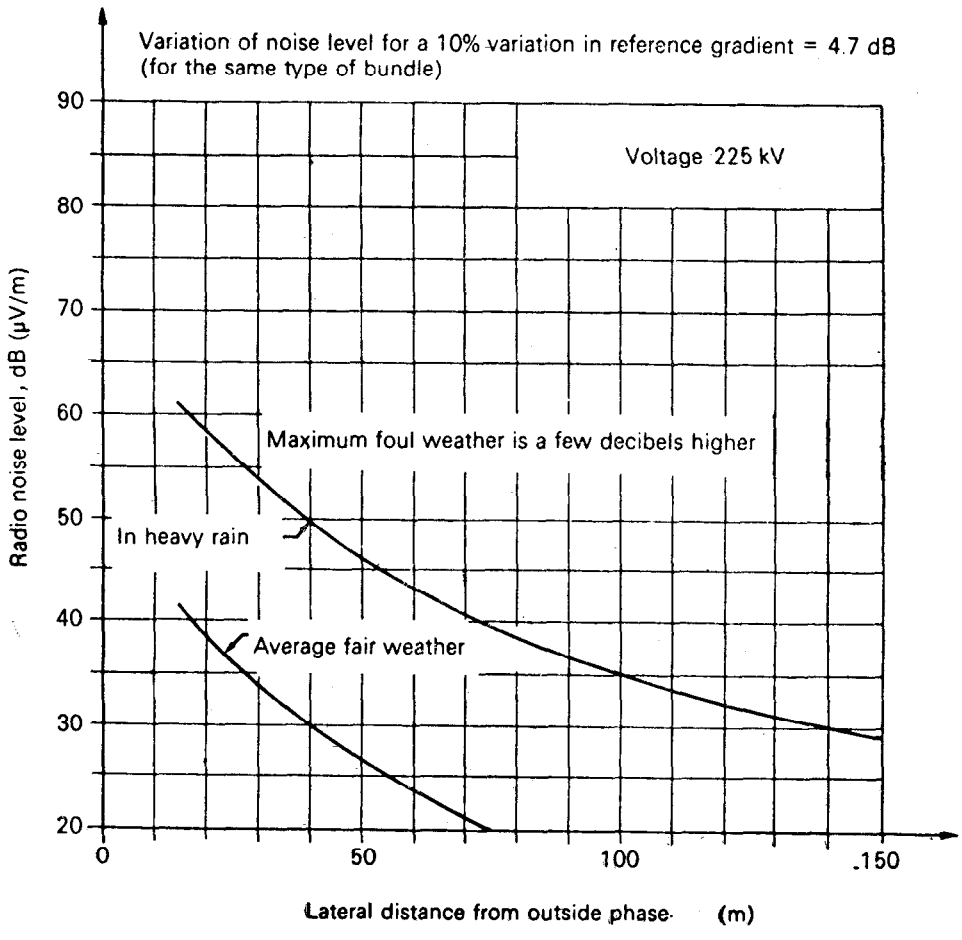

FIG. 3. — Flat formation.

Line 225 kV

Frequency 0.5 MHz	Conductors				Maximum gradients			
H min. 11 m 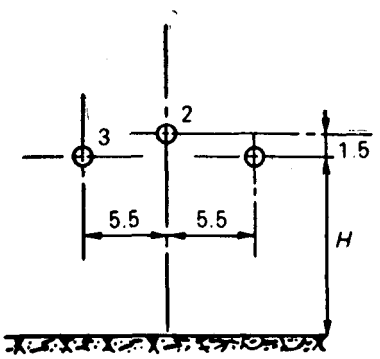	Number of conductors	Phase spacing *S* (m)	Radius of bundle *R* (mm)	Radius of conductor *r* (mm)	Phase 1 (kV eff /cm)	Phase 2 (kV eff /cm)	Phase 3 (kV eff /cm)	Level correction (dB)
	1	5.5	–	13.2	15.55	16.45	15.55	0
	1	5.5	–	15.5	13.60	14.40	13.60	–6
	1	5.5	–	16.2	13.10	13.90	13.10	–7.6

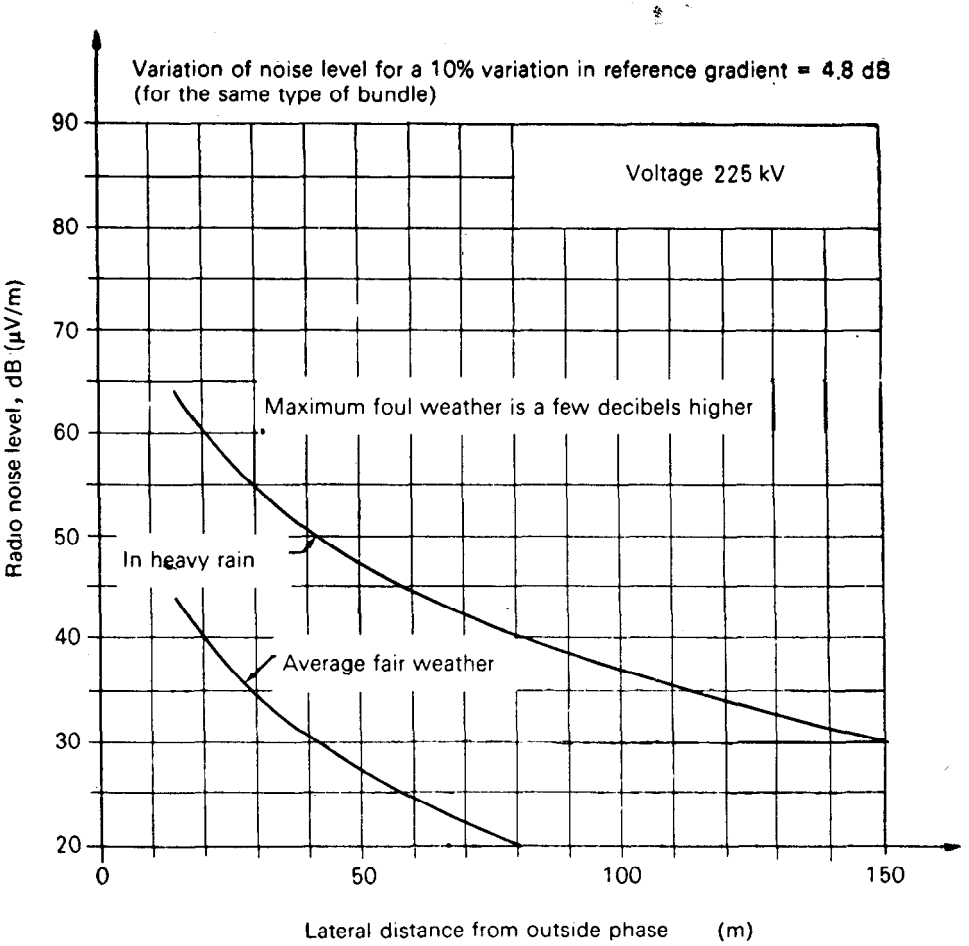

FIG. 4 — Arched formation.

Line 225 kV

Frequency 0.5 MHz	Conductors				Maximum gradients			
H min. 11 m 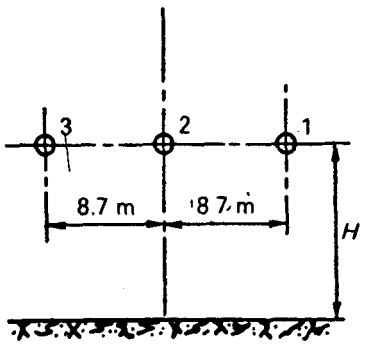	Number of conductors	Phase spacing S (m)	Radius of bundle R (mm)	Radius of conductor r (mm)	Phase 1 (kV eff /cm)	Phase 2 (kV eff /cm)	Phase 3 (kV eff /cm)	Level correction (dB)
	1	8.7	–	13.2	14.60	15.45	14.60	0
	1	8.7	–	15.5	12.75	13.50	12.75	–6.3
	1	8.7	–	16.2	12.30	13.00	12.30	–8.0

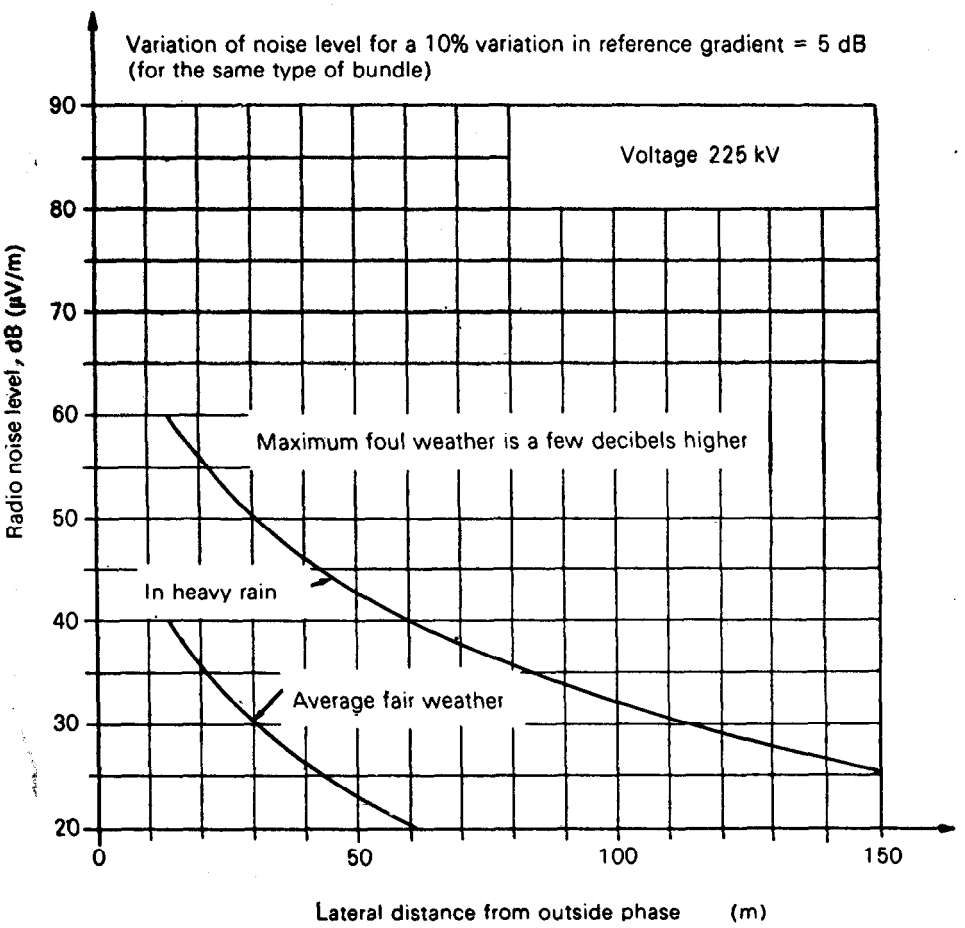

FIG. 5 — Flat wide formation.

Line 362 kV

Frequency 0.5 MHz	Conductors				Maximum gradients			
H min. 10,0 m 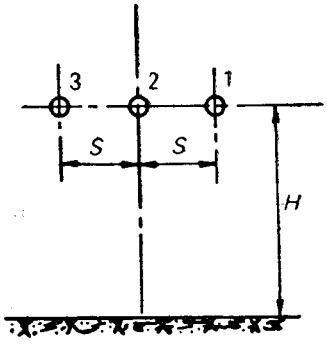	Number of conductors	Phase spacing *S* (m)	Radius of bundle *R* (mm)	Radius of conductor *r* (mm)	Phase 1 (kV eff /cm)	Phase 2 (kV eff /cm)	Phase 3 (kV eff /cm)	Level correction (dB)
	1	9.75	–	20.35	16.1	17.0	16.1	0
	2	9.0	–	13.4	16.7	17 8	16.7	–4

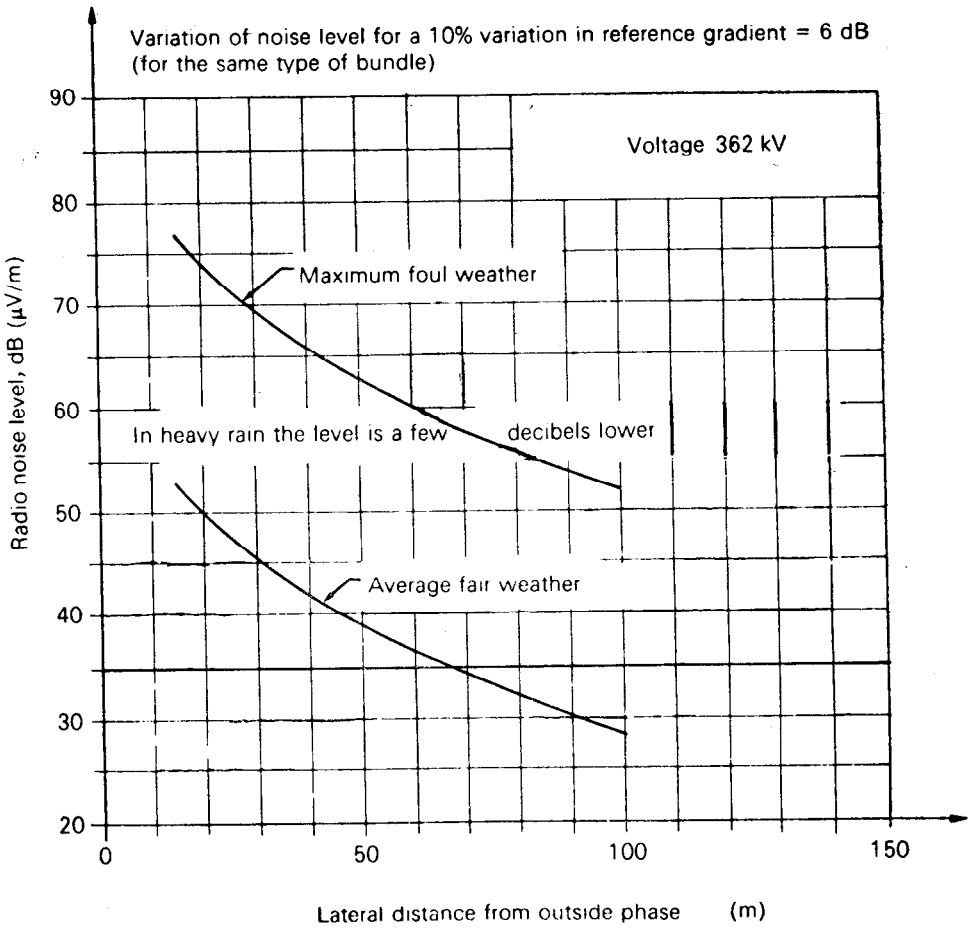

FIG 6 — Flat formation.

Line 380 kV

Frequency 0.5 MHz

H min. 12 m

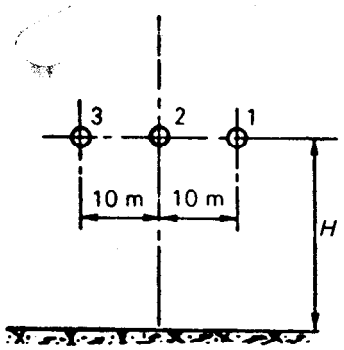

Conductors				Maximum gradients			
Number of conductors	Phase spacing *S* (m)	Radius of bundle *R* (mm)	Radius of conductor *r* (mm)	Phase 1 (kV eff /cm)	Phase 2 (kV eff /cm)	Phase 3 (kV eff /cm)	Level correction (dB)
2	10,0	200	13.2	17.20	18.50	17.20	0
2	10,0	200	15.5	15.05	16.20	15.05	−5.5
2	10,0	200	16.2	14.50	15.60	14.50	−7.0
1	10,0	–	22.4	15.50	16.40	15.50	+6.5

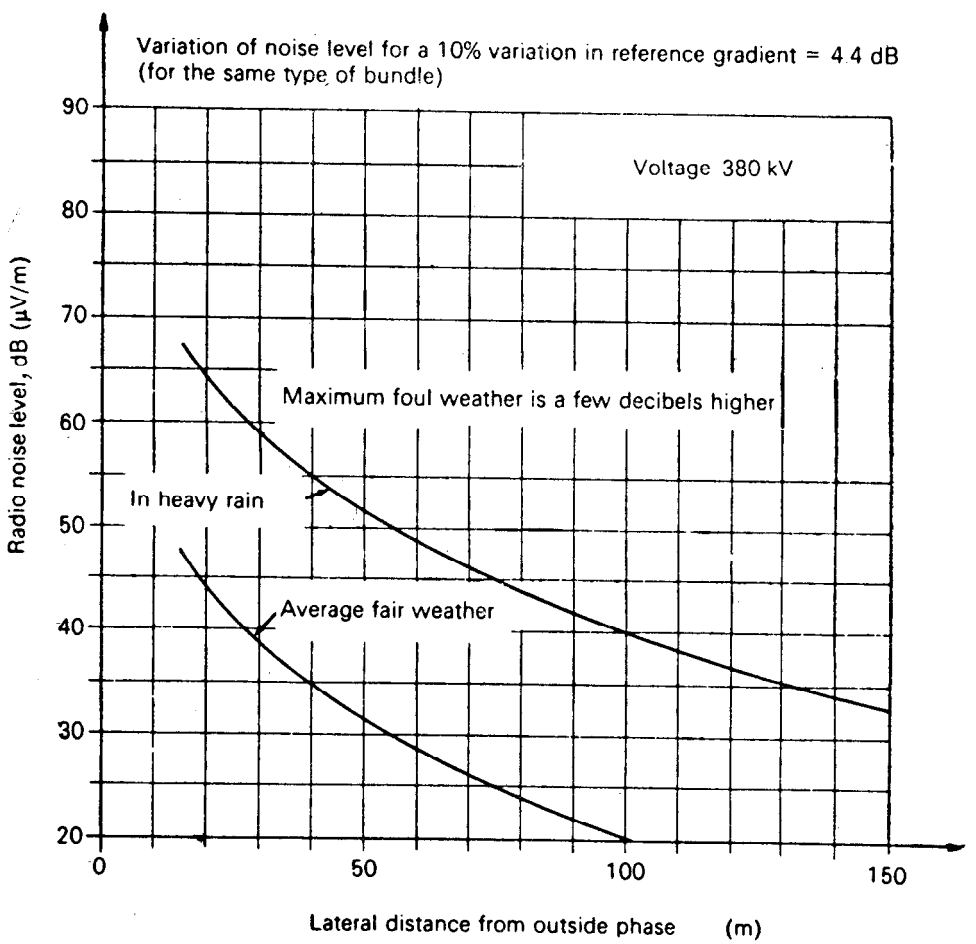

FIG. 7. — Flat formation.

Line 380 kV

Frequency 0.5 MHz	Conductors				Maximum gradients			
H min. 12 m 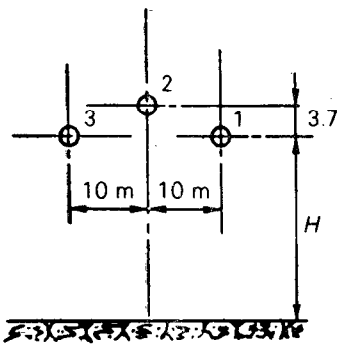	Number of conductors	Phase spacing *S* (m)	Radius of bundle *R* (mm)	Radius of conductor *r* (mm)	Phase 1 (kV eff /cm)	Phase 2 (kV eff /cm)	Phase 3 (kV eff /cm)	Level correction (dB)
	2	10.00	200	13.2	17.20	18.00	17.20	0
	2	10.00	200	15.5	15.05	15.75	15.05	−5.5
	2	10.00	200	16.2	14.60	15.30	14.60	−6.7
	1	10.00	–	22.4	15.50	16.00	15.50	+6.7

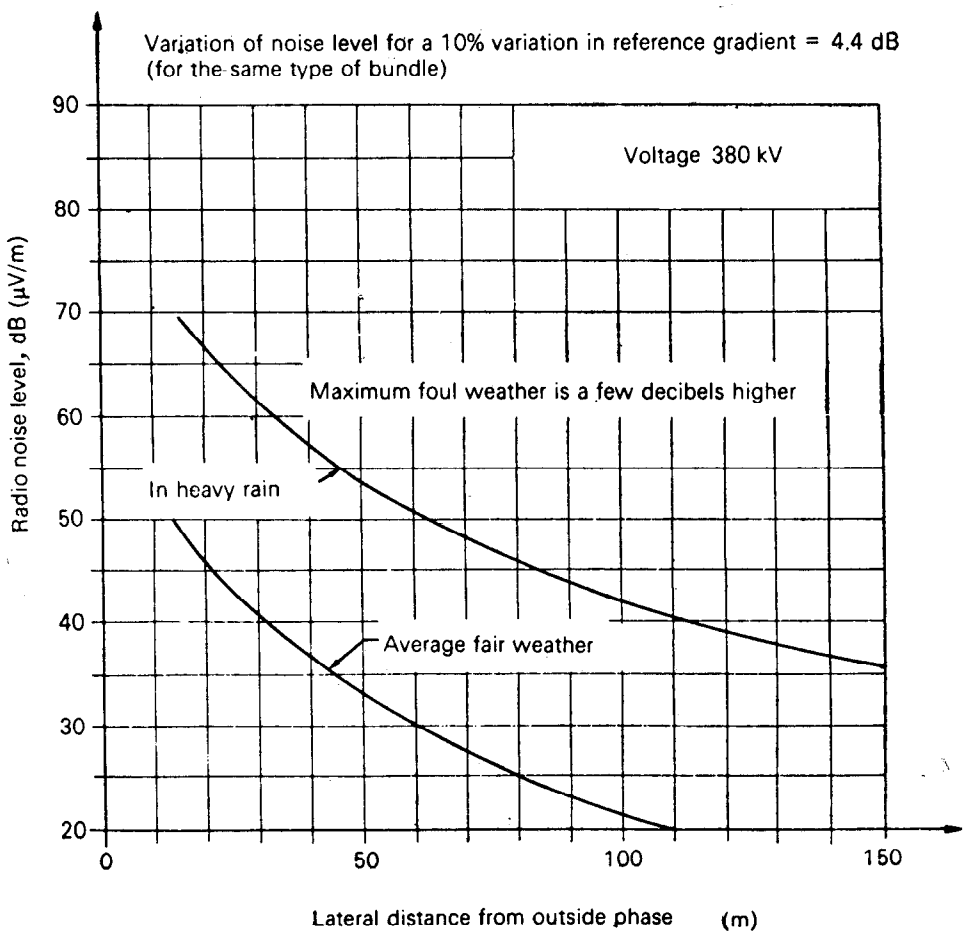

FIG. 8. — Arched formation.

Line 525 kV

Frequency 0.5 MHz	Conductors				Maximum gradients			
H min. 12 m 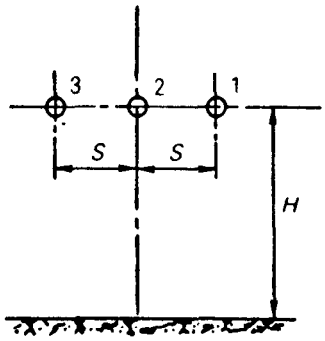	Number of conductors	Phase spacing *S* (m)	Radius of bundle *R* (mm)	Radius of conductor *r* (mm)	Phase 1 (kV eff./cm)	Phase 2 (kV eff./cm)	Phase 3 (kV eff./cm)	Level correction (dB)
	4	12.2	323	10.80	17.9	19.3	17.9	0
	3	9.2	264	14.80	17.3	19.0	17.3	+1
	2	9.1	229	20.95	16.5	17.9	16.5	+7

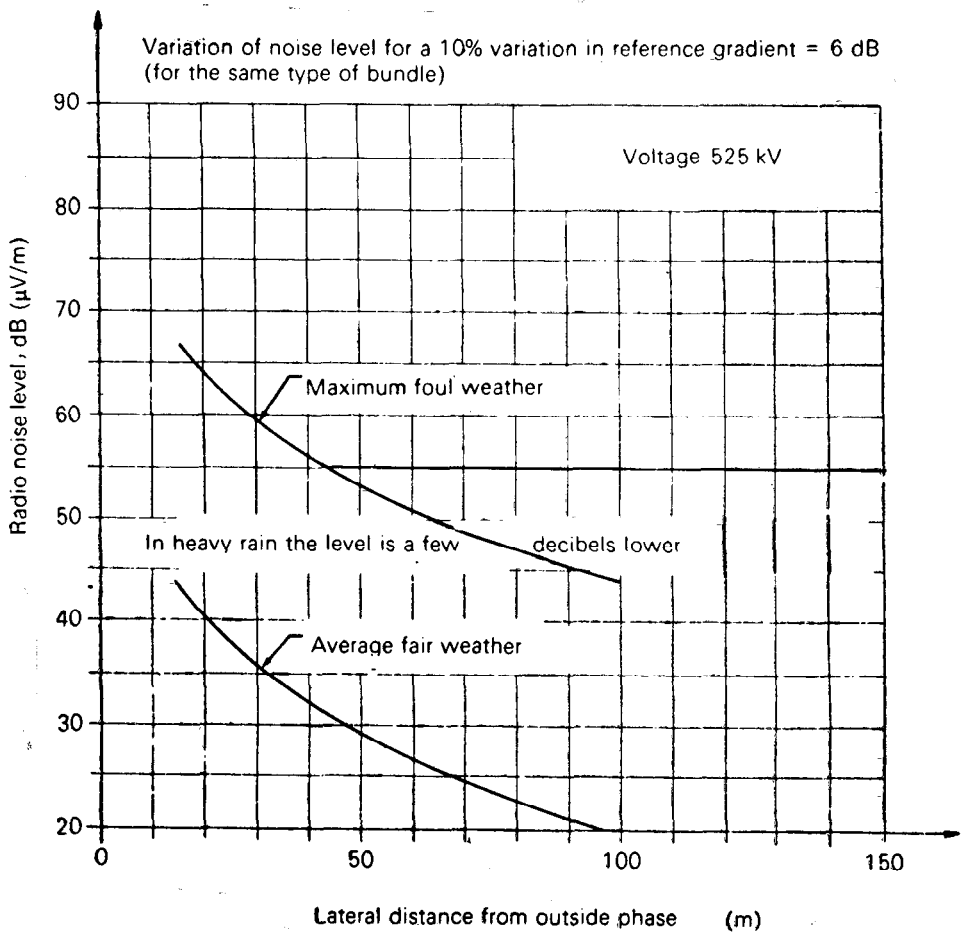

FIG. 9. — Flat formation.

Line 750 kV

Frequency 0.5 MHz

H moy 18 m
H min. 14 m

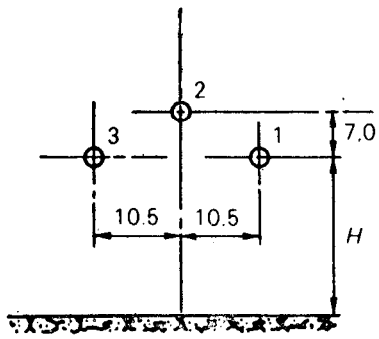

Conductors				Maximum gradients			Level correction
Number of conductors	Phase spacing *S* (m)	Radius of bundle *R* (mm)	Radius of conductor *r* (mm)	Phase 1 (kV eff /cm)	Phase 2 (kV eff /cm)	Phase 3 (kV eff /cm)	(dB)
4	10.5	212	15.5	18.30	17.00	18.30	0
4	10.5	212	18.95	15.70	14.60	15.70	−4.9
4	10.5	323	15.5	18.40	17.05	18.40	+0.8
4	10.5	323	18.95	15.65	14.50	15.65	−4.7

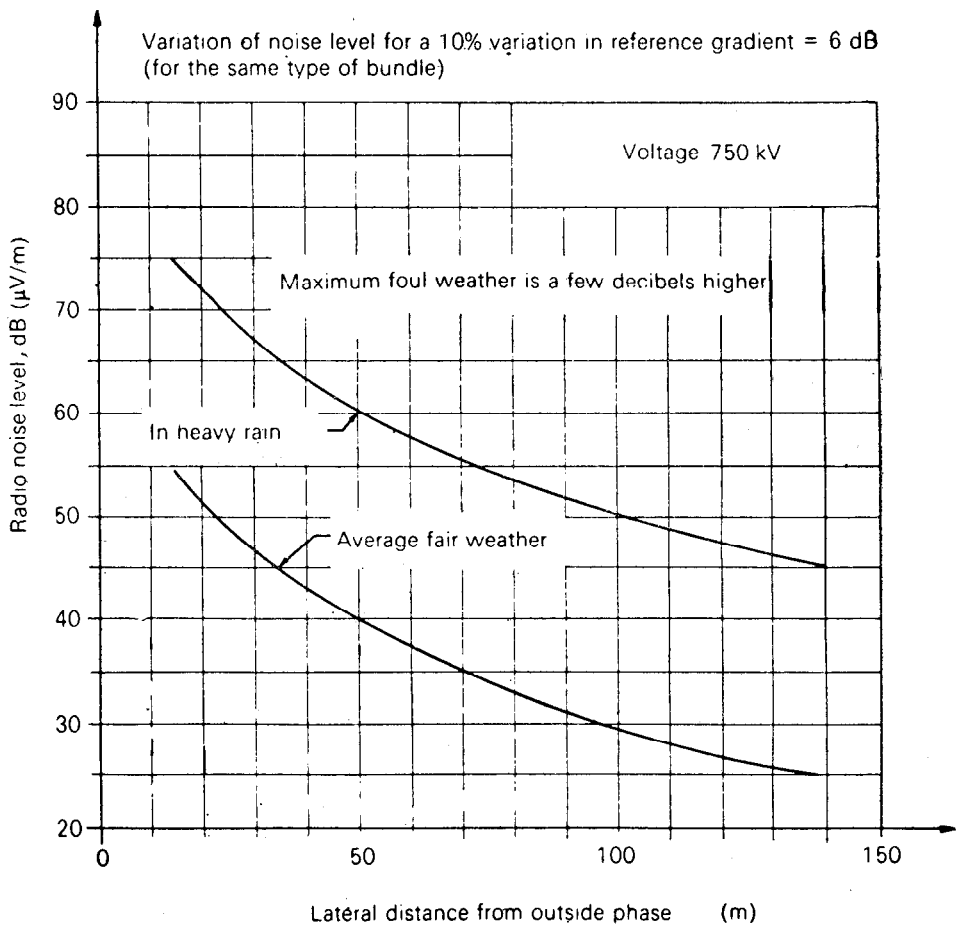

FIG 10 – Arched formation

Line 765 kV

Frequency 0.5 MHz	Conductors				Maximum gradients			
H min. 14 m 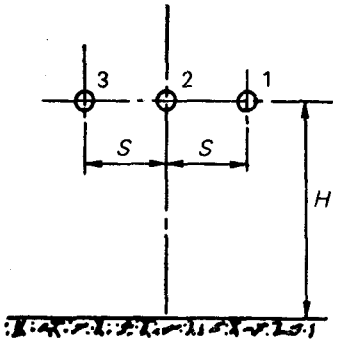	Number of conductors	Phase spacing *S* (m)	Radius of bundle *R* (mm)	Radius of conductor *r* (mm)	Phase 1 (kV eff /cm)	Phase 2 (kV eff /cm)	Phase 3 (kV eff /cm)	Level correction (dB)
	4	15.2	323	17.55	16.9	18.0	16.9	0
	4	13.7	323	15.19	19.2	20.6	19.2	+6.0

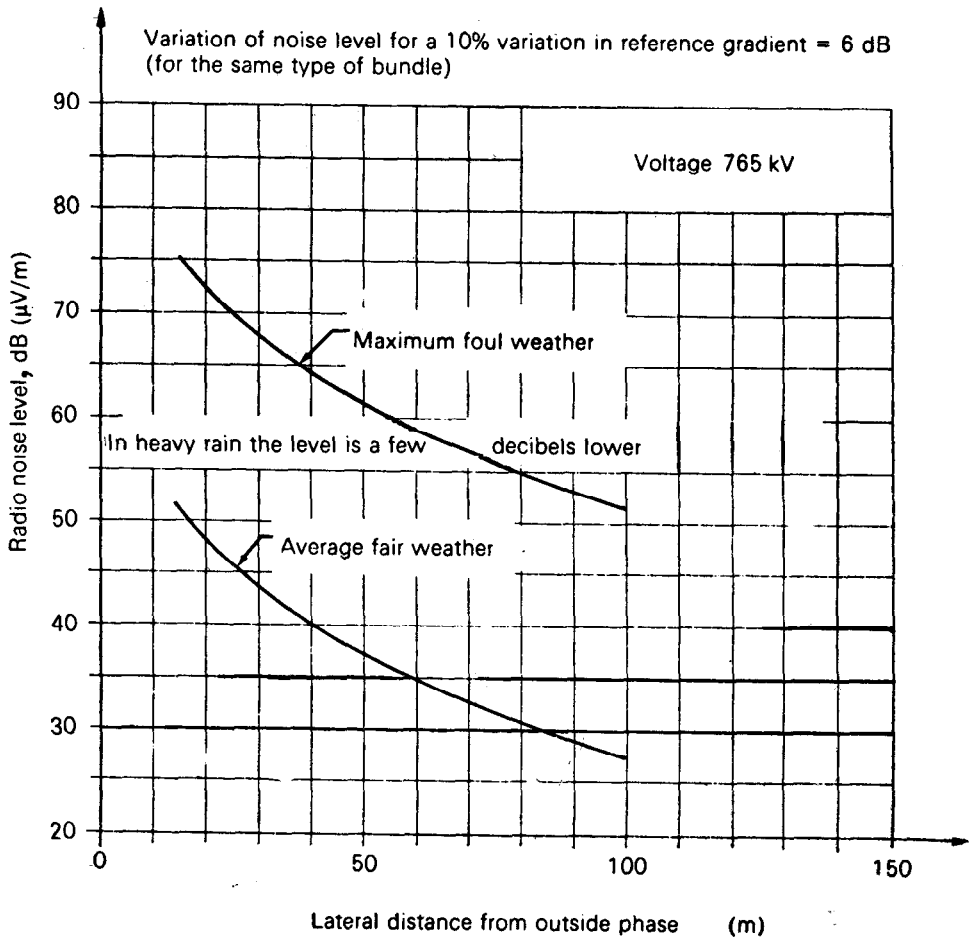

FIG. 11 — Flat formation.

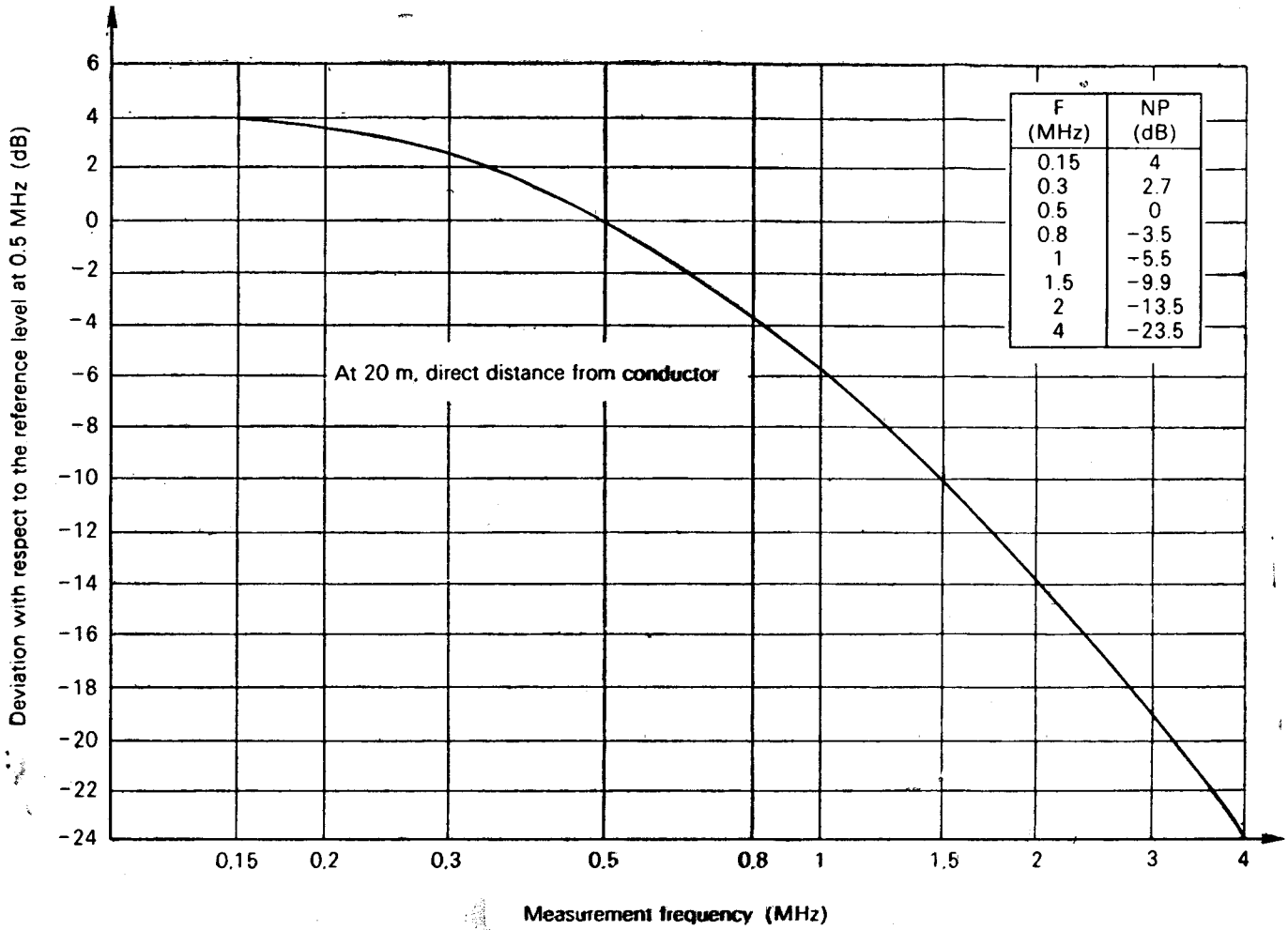

FIG. 12. — Typical frequency spectra for the radio noise fields of high voltage power lines.

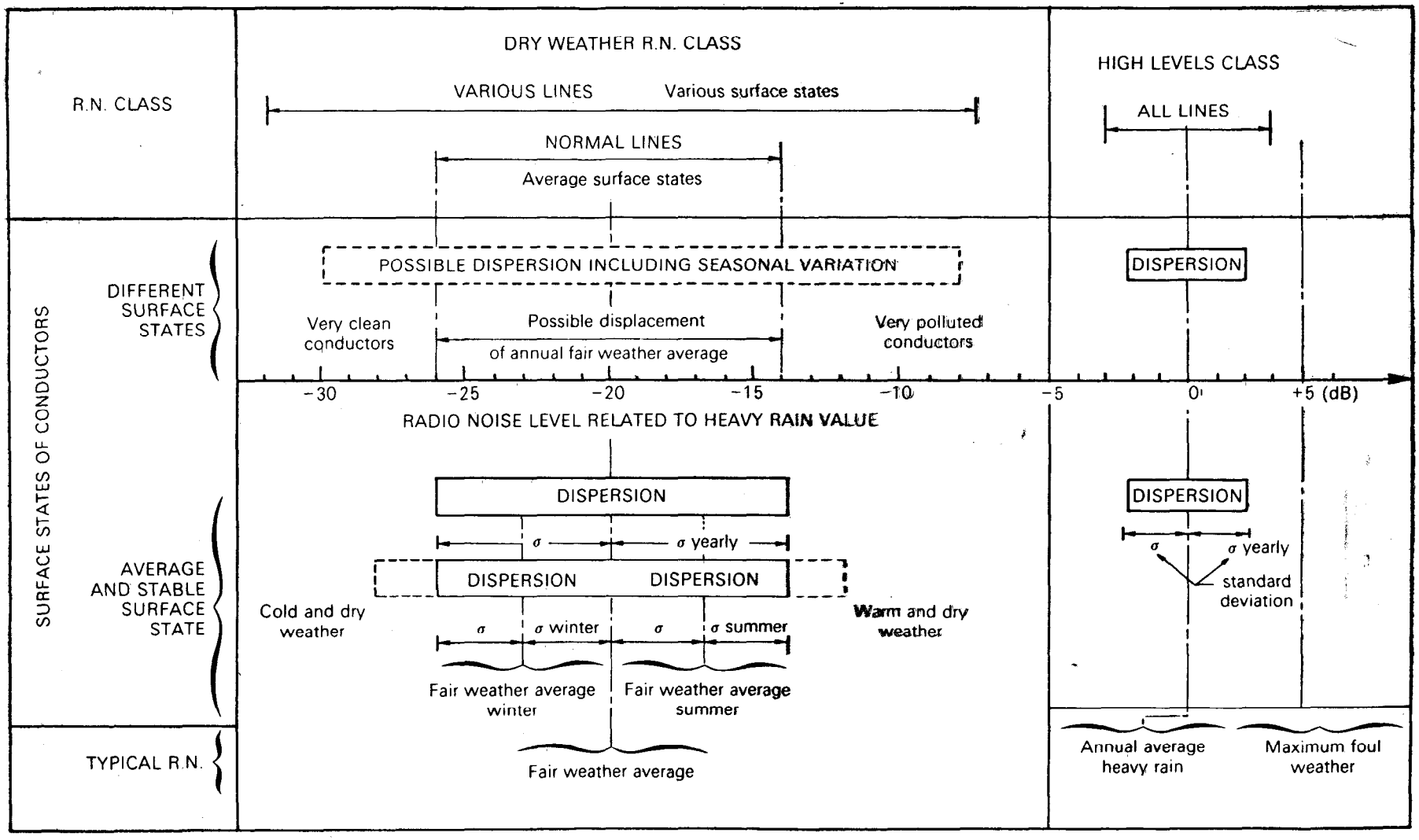

NOTE — Daily dry weather variations are not included in this graph.

FIG. 13 — Prediction of radio noise level of a transmission line for various types of weather.

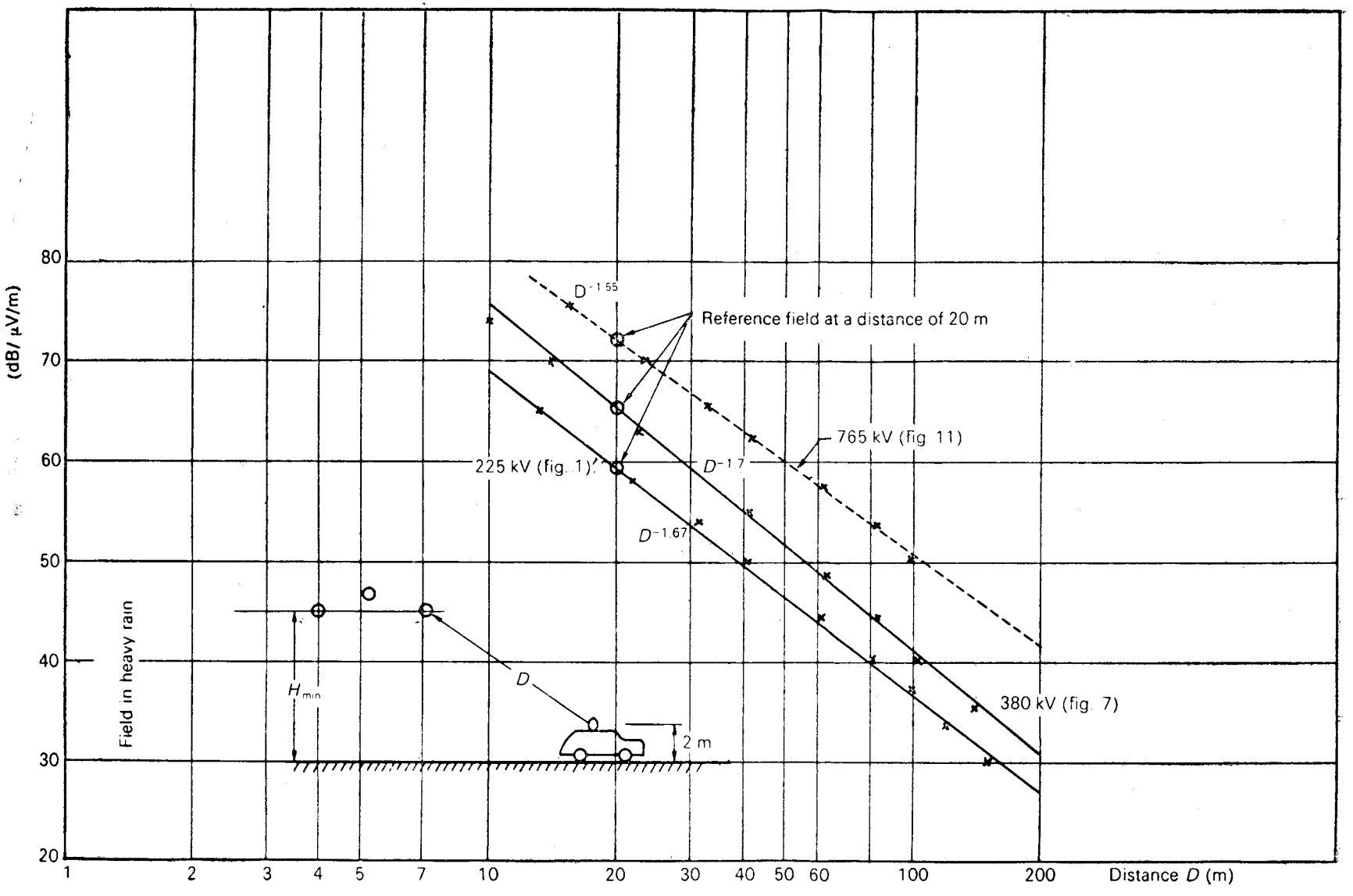

FIG. 14. — Examples of transformations of profiles of Fig1 to 11.